EasyChair Preprint

№ 6643

Developing a Dynamic Diesel Engine Model for Energy Optimal Control

Viktor Leek and Lars Eriksson

September 21, 2021

Developing a Dynamic Diesel Engine Model for Energy Optimal Control

Viktor Leek, Lars Eriksson

Division of Vehicular Systems, Linköping University, Sweden
viktor.leek@liu.se, lars.eriksson@liu.se

Abstract

A dynamic heavy-duty Euro 6 diesel engine model for energy optimal control is developed. The modeling focus is on accuracy in the entire engine operating range, with attention to the region of highest efficiency and physically plausible extrapolation. The effect of the air-to-fuel ratio on combustion efficiency is studied, and it is demonstrated how this influences the energy optimal transient control. A convenient, physics-based, method for pressure sensor bias estimation is also presented.
Keywords: Diesel engine modeling, Optimal control

1 Introduction

Economy, climate, and diesel engines. Ever since the breakthrough of Rudolph Diesel's engine it has been impossible to consider the first two without the third, and the machine is now one of the two prime movers of globalization (Smil, 2017). As its position in the global economy has risen to the predominant one, so has its impact on the climate. And while it might be possible to imagine a future transportation system without diesel engines, it is impossible to imagine a transition to that system without large investments, so the continued development of the diesel engine is perhaps more important than ever. By reducing fuel consumption, improving emissions, enabling renewable fuels, and increasing reliability, it is possible to improve, individually and in combination, the economy, and the climate. This work aims to help in that effort by developing a diesel engine model for energy optimal control.

The model's intended use is to study the effect of the turbocharger selection on the energy optimal control of the air- and fuel-path of a heavy-duty Euro 6 diesel engine. While being the reason *why* this work is conducted, it is *not* the only area of use. Models are only approximations of reality, and for them to be useful to others it is necessary to show what aspects of reality they reflect, and how accurately they do it. Here, this is done in two parts. This first part describes the development of the model, which include determining the needed properties and settling on the equations. The second part consists of parametrization and validation and is found in (Ekberg et al., 2018).

The contributions include the development of a diesel engine model for studying the turbocharger effect on the energy optimal control, with a novel inclusion of the air-to-fuel ratio effect on the engine efficiency, and is available as open-source (Leek et al.). Another important contribution is a physics-based method for estimating pressure sensor bias in experimental data.

The paper is outlined as follows. Section 2 introduces the subject of modeling for energy optimal control, Section 3 presents the data used for modeling and the method for estimating pressure sensor bias, Section 4 describes the model development, Section 5 demonstrates the energy optimal control of the model, and Section 6 presents the conclusions.

2 Modeling for Energy Optimal Control

With the intention of using the model for energy optimal control, it is necessary to investigate the implications of this on the modeling work. To do that, a basic discussion on optimal control problems, and their numerical solution, is needed.

2.1 Optimal control

An optimal control problem (OCP) can be formulated as:

$$\begin{aligned} \min_{u} \quad & E(t_f, x(t_f)) + \int_0^{t_f} L(t,x,u)\, dt \\ \text{s.t.} \quad & \dot{x} = f(t,x,u),\ t \in [0,t_f], \\ & x(0) \in \mathscr{X}_0, \\ & x(t) \in \mathscr{X},\ t \in [0,t_f], \\ & u(t) \in \mathscr{U},\ t \in [0,t_f], \\ & x(t_f) \in \mathscr{X}_f \end{aligned} \tag{1}$$

The problem consists of finding the optimal control, u^*, and the state trajectory, x^*, that minimize the cost function and does not violate the constraints. The problem's defining characteristic is the differential constraint $\dot{x} = f(t,x,u)$. The objective function consists of two parts. An integral cost $\int L(t,x,u)\, dt$, and a terminal cost $E(t_f, x(t_f))$. There are constraints on the initial value, $x(0) \in \mathscr{X}_0$, path constraints $x(t) \in \mathscr{X}$ and $u(t) \in \mathscr{U}$, and constraints on the final state $x(t_f) \in \mathscr{X}_f$.

2.2 Numerical solution to optimal control problems

There exist several approaches for solving optimal control problems numerically, and an overview can be found in (Rao, 2009). This work focuses on direct methods. They are the most popular methods in general (Diehl et al., 2006), and have proved successful in the optimal control of diesel engines (Asprion et al., 2014; Sivertsson and Eriksson, 2014; Mancini, 2014).

Direct methods are characterized by first discretizing the OCP and turning it into a nonlinear program (NLP), solving that numerically, and then reconstructing the OCP solution from the NLP one. The process of casting the OCP as a NLP is known as transcription. Transcription methods consider some form of grid on which the solution is parameterized. A common, and the most basic of which, is a fixed, equidistant, grid

$$0 = t_0 < t_1 < \cdots < t_{N-1} < t_N = t_f \tag{2a}$$

$$h = t_{n+1} - t_n,\ n = 0, 1, \ldots, N-1 \tag{2b}$$

where h is the fixed step length, and N the number of intervals. The control signal is typically constant over each segment (Diehl, 2011), and consistent with a zero-order hold control system implementation. The state trajectory differs between the individual direct methods, but the two most popular, direct multiple shooting and direct collocation (Diehl et al., 2006), integrate the dynamics separately on each segment, forming a discontinuous trajectory, which is made continuous by introducing defect constraints (Betts, 2010). Based on this, the number of NLP variables resulting from using the direct multiple shooting method is calculated as $Nn_u + (N+1)n_x$, where n_x is the number of states, and n_u the number of control inputs (Andersson, 2013). The corresponding metric for the direct collocation method is $Nn_u + (N(n_{cp}+1)+1)n_x$ where n_{cp} is the number of collocation points. Considering how the NLP variables scale with the number of states and controls, it is preferable that the number of states and controls is kept low, otherwise the NLP risks being too difficult or too expensive to solve, which defeats the purpose.

Literature on optimal control of diesel engines (Asprion et al., 2014) suggests a large NLP, with potentially tens of thousands of variables. To solve that efficiently it is desirable to use a gradient based solver of Newton-type which uses first and second derivatives. As nothing is known of the objective or constraints at the time of modeling, constraints must be passed on to the model. The state trajectory is therefore made, at least, two times differentiable. This has the positive side-effect to aid simulations, as initial value problem solvers assume a sufficiently smooth solution (Ascher and Petzold, 1998).

Based on the characteristics of an optimal solution (Nocedal and Wright, 2006; Asprion et al., 2014), the solution lies at the border of the allowable set and/or in the unconstrained optimum. This has two implications on the modeling work. The first, that the model needs physically plausible extrapolation properties to capture the full set of operating conditions. The second, that the model fit needs to be good in the region of best efficiency, where optimum is expected to be found.

2.3 Modeling implications

Optimization-oriented models need to be *accurate* in order to capture a large set of operating conditions, *small*, for efficient evaluation, provide *plausible extrapolation*, to capture solutions at the border of the feasible set, and be implementable using only *standard mathematical operations*, for algorithmic differentiation applicability. Models for energy optimal control also need *high accuracy in the region of best efficiency*. To successfully meet these demands, it is necessary to combine an approach based on first principles and phenomenology. By formulating the dominating equations from first principles the model is restricted in size, and extrapolation is physically plausible. The phenomenological part consists of, based on available data, determining how the equation parameters change with the operating conditions, and is fundamental to good accuracy over a large operating range.

With the intended use of studying the turbocharger impact on the energy optimal control, it is important with a good model of the turbocharger as it gives rise to the dominating dynamics on the air and fuel path, but also with a good model of its implicit effects on the said path. Larger turbines produce a lower backpressure, which decreases pumping work and thereby increases efficiency (Eriksson et al., 2002). Its larger size also means an increased inertia. This hampers the engine's transient response, and therefore the air-to-fuel ratio is lower during transients. Low air-to-fuel ratio lowers combustion efficiency (Heywood, 1988; Eriksson and Nielsen, 2014), so in order to study the turbocharger impact on the energy optimal control it is necessary to include this effect in the model.

3 Data

Five datasets are used to guide the modeling, and a listing is found in Table 1. Dataset A consists of engine dynamometer experimental data collected in an engine test cell. Dataset B is high-fidelity simulation data from a GT-Power (Gamma Technologies, 2004) model of the engine. Dataset C is a compressor map formed by running measurements in a turbocharger gas stand. Dataset D is a turbine map, also collected from gas stand measurements. Dataset E is data on the throttle area as a function in throttle angle.

The datasets fulfill different aspects of the modeling work. In particular, the high-fidelity simulation data, B, is used instead of cylinder pressure data, which is not available. The simulation data contains information on the torque components, which makes it possible to model the cylinder in better detail than what is possible if only dataset A is used. How the different datasets are fused is found in the validation and parametrization part of this

Table 1. Datasets used to find model parameters.

Dataset	Signals	Samples
A. Engine dynamometer experimental data.	24	235
B. GT Power high-fidelity simulation data.	22	160
C. Compressor map - Gas stand measurements.	4	73
D. Turbine map - Gas stand measurements.	4	73
E. Throttle area - Measurements of angle versus area.	1	11

work (Ekberg et al., 2018).

3.1 Pressure offset estimation

An important part in modeling is having access to reliable data. Unfortunately, measurements contain errors to some degree. Here, dataset A contains bias in the pressure sensors on the intake side. This is compensated for by estimating it. The estimation is based on the observation that flow squared is proportional to the pressure drop over a restriction. By denoting the upstream pressure and temperature by p_{us} and T_{us} respectively, the downstream pressure by p_{ds}, the bias in that sensor by p_{bias}, and the flow by W, the relation is formulated as

$$(p_{\text{us}} - (p_{\text{ds}} + p_{\text{bias}}))\frac{p_{\text{us}}}{\sqrt{T_{\text{us}}}} \propto W^2$$

Rearranging the equation, and introducing the proportionality constant c, the following least squares problem is solved to estimate the bias:

$$\left[p_{\text{us}}/\sqrt{T_{\text{us}}},\ W^2\right]\begin{bmatrix} p_{\text{bias}} \\ c \end{bmatrix} = (p_{\text{us}} - p_{\text{ds}})\frac{p_{\text{us}}}{\sqrt{T_{\text{us}}}} \tag{3}$$

4 Model

With the model's intended use in mind, a mean value modeling approach is taken. This considerably reduces the model size, when compared to a 1D model, while still being able to capture the relevant quantitative properties of the air and fuel path.

In this work, a model of the throttle is included. The purpose of this is to extend the model's area of use by making it possible to connect it to an aftertreatment system model. As aftertreatment systems are sensitive to temperature, there is a need to control airflow through the system to avoid unnecessary cooling. This means that the model has an extra control volume before the throttle, which means one extra pressure state (boost pressure). Users that do not need this feature can remove it.

4.1 Dynamics

The model is governed by four scalar ODEs: boost pressure dynamics, intake manifold pressure dynamics, exhaust manifold pressure dynamics, and the dominating one, turbocharger rotational dynamics.

The modeling of the control volumes is based on differentiation of the ideal gas law, an isothermal assumption, which means no temperature change in the system, and assumption of mass conservation. The modeling follows (Eriksson and Nielsen, 2014).

Denote the volumes by V, pressures by p, temperatures by T, and let dot notation be used to denote differentiation with respect to time. Introduce the subscript b (boost) for the volume before the throttle, im for the intake manifold, and em for the exhaust manifold. Let R_{a} be the gas constant of air, and R_{e} the gas constant of exhaust gas. Introduce the compressor flow as W_{c}, the throttle flow as W_{thr}, the flow into the cylinders as W_{cyl}, the fuel flow as W_{f}, the turbine flow as W_{t}, and the wastegate flow as W_{wg} (see Figure 2 for an overview). The flows are defined later. The filling and emptying dynamics of the control volumes is then expressed as

$$V_{\text{b}}\dot{p}_{\text{b}} = R_{\text{a}}T_{\text{b}}(W_{\text{c}} - W_{\text{thr}}) \tag{4a}$$
$$V_{\text{im}}\dot{p}_{\text{im}} = R_{\text{a}}T_{\text{im}}(W_{\text{thr}} - W_{\text{cyl}}) \tag{4b}$$
$$V_{\text{em}}\dot{p}_{\text{em}} = R_{\text{e}}T_{\text{em}}(W_{\text{cyl}} + W_{\text{f}} - W_{\text{t}} - W_{\text{wg}}) \tag{4c}$$

The model builds on the isothermal assumption and should be tested. Figure 1 shows the intake manifold temperature and ambient temperature of dataset A. The data shows a consistent 2 % temperature increase, relative to ambient, which is considered small. This motivates two modeling simplifications, isothermal control volumes, and ideal charge air cooler. Should it be desirable, the intake manifold temperature can be set to 2% above ambient. Furthermore, literature (Wahlström and Eriksson, 2011) suggest only minor differences in observed behavior when using an adiabatic model of the control volumes with temperature state, which further motivates the decision to not include temperature dynamics.

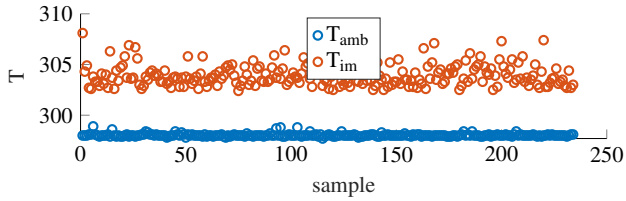

Figure 1. Ambient and intake manifold temperature from dataset A.

Modeling of the turbocharger dynamics follows from Newton's second law of motion. To formulate the equation ω is used to denote angular velocity, J to denote moment of inertia, and subscript tc is used for the turbocharger. The effects of the turbine and compressor on the dynamics is expressed in terms of their power. $P_{\text{t}}\eta_{\text{m}}$ is used to denote the turbine power and includes mechanical efficiency, and P_{c} is the compressor power. To obtain torque, power is divided by angular velocity, which means that the model is only valid for positive velocities. The

turbocharger dynamics is formulated as:

$$J_{\mathrm{tc}}\dot{\omega}_{\mathrm{tc}} = \frac{P_{\mathrm{t}}\,\eta_{\mathrm{m}} - P_{\mathrm{c}}}{\omega_{\mathrm{tc}}} \tag{5}$$

With the dynamics presented, it can be concluded that the model has four states x:

$$x = [p_{\mathrm{b}}, p_{\mathrm{im}}, p_{\mathrm{em}}, \omega_{\mathrm{tc}}]^{\mathrm{T}} \tag{6}$$

and to control these, there are three control inputs u. The fuel injection per cycle and cylinder u_{f}, the throttle effective area u_{thr}, and the wastegate effective area u_{wg}:

$$u = [u_{\mathrm{f}}, u_{\mathrm{thr}}, u_{\mathrm{wg}}]^{\mathrm{T}} \tag{7}$$

The engine speed, N_{ice}, is an external input in the model and a model overview is found in Figure 2.

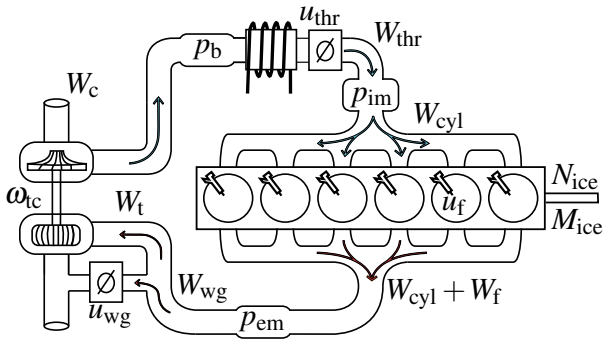

Figure 2. Model overview. Shown are the four states: boost pressure p_{b}, intake manifold pressure p_{im}, exhaust manifold pressure p_{em}, and turbocharger angular velocity ω_{tc}, and the three control inputs: Fuel injection per cycle and cylinder u_{f}, throttle effective area u_{thr}, and wastegate effective area u_{wg}. Also shown are the flows, W, in the model.

4.2 Throttle

Modeling of the throttle follows (Eriksson and Nielsen, 2014), where an isentropic compressible restriction is used. To describe the model, further notation is needed. $A_{\mathrm{thr,max}}$ is the throttle maximum area, $C_{\mathrm{D,thr}}$ the flow coefficient, Ψ_{thr} flow parameter, and the flow is calculated as

$$W_{\mathrm{thr}} = \frac{p_{\mathrm{b}}}{\sqrt{R_{\mathrm{a}}\,T_{\mathrm{b}}}} C_{\mathrm{D,thr}}\,A_{\mathrm{thr,max}}\,u_{\mathrm{thr}}\,\Psi_{\mathrm{thr}} \tag{8}$$

The effective throttle area $A_{\mathrm{thr,max}}\,u_{\mathrm{thr}}$ is linear in the control input. This is not in accordance with dataset E. Data suggest a cubic relation, but since the relation is injective, the actual control input can be reconstructed from the effective area. So, to avoid nonlinearity, effective area is modeled as linear in the artificial control input u_{thr}.

(Holmbom and Eriksson, 2018) compares different compact models for the flow parameter Ψ_{thr}. Good performance is obtained for the model (Shen and Ohata, 2011), which is based on the conservation of mass, energy, and momentum. By denoting the ratio of specific heats by γ_{a}, and the pressure ratio by Π_{thr}, the model can be expressed as:

$$\Psi_{\mathrm{thr}} = \sqrt{\frac{\gamma_{\mathrm{a}}+1}{2\gamma_{\mathrm{a}}}(1-\Pi_{\mathrm{thr}})\left(\Pi_{\mathrm{thr}} + \frac{\gamma_{\mathrm{a}}-1}{\gamma_{\mathrm{a}}+1}\right)} \tag{9a}$$

$$\Pi_{\mathrm{thr}} = \begin{cases} \frac{p_{\mathrm{im}}}{p_{\mathrm{b}}} & \text{if } \frac{p_{\mathrm{im}}}{p_{\mathrm{b}}} \geq \frac{1}{\gamma_{\mathrm{a}}+1} \\ \frac{1}{\gamma_{\mathrm{a}}+1} & \text{otherwise} \end{cases} \tag{9b}$$

The saturation of flow gives rise to the conditional expression. It does not have a continuous derivative. To circumvent that, the logistic function is used to make the derivative continuous, at the cost of nonlinearity and parametrization effort:

$$\Pi_{\mathrm{thr}} = \Pi^{\mathrm{choke}} + c_{\mathrm{switch}}(\Pi - \Pi^{\mathrm{choke}}) \tag{10a}$$

$$c_{\mathrm{switch}} = 1/\left(1 + e^{-c_\Psi(\Pi - \Pi^{\mathrm{choke}})}\right) \tag{10b}$$

$$\Pi^{\mathrm{choke}} = 1/(\gamma_{\mathrm{a}}+1) \tag{10c}$$

$$\Pi = p_{\mathrm{im}}/p_{\mathrm{b}} \tag{10d}$$

The model contains one tuning parameter, c_Ψ, which determines the steepness of the switch.

4.3 Cylinder

The cylinder air mass flow is based on the modeling of the volumetric efficiency and follows the approach in (Heywood, 1988). By denoting the volumetric efficiency by η_{vol}, the engine displacement by V_{D}, and the engine speed by N_{ice}, the air mass flow is calculated as

$$W_{\mathrm{cyl}} = \eta_{\mathrm{vol}}\frac{2V_{\mathrm{D}}\,p_{\mathrm{im}}}{R_{\mathrm{a}}\,T_{\mathrm{im}}N_{\mathrm{ice}}} \tag{11}$$

The question is how to model volumetric efficiency. A common approach is to base the model on intake manifold pressure and engine speed (Heywood, 1988). The primary modeling dataset, A, does not show such a dependence, see Figure 3, nor does it show a clear correlation with any other variable in the dataset, why constant volumetric efficiency is used.

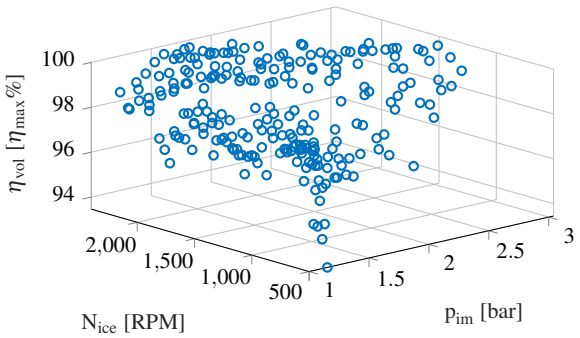

Figure 3. Volumetric efficiency, in circles, relative to the maximum value. Plotted against engine speed and intake manifold pressure.

The fuel mass flow is calculated as $W_{\mathrm{f}} = n_{\mathrm{cyl}}N_{\mathrm{ice}}\,u_{\mathrm{f}}/2$ and the fuel-to-air equivalence ratio ϕ is calculated as

$\phi = \mathrm{AF_s}\, W_\mathrm{f}/W_\mathrm{cyl}$, where $\mathrm{AF_s}$ is the air-to-fuel stoichiometric ratio. The air-to-fuel equivalence ratio $\lambda = 1/\phi$ is typically used by control engineers instead of ϕ. However, in the model it is preferable to use ϕ as it is not singular for zero fuel flow.

Cylinder out temperature modeling follows (Sivertsson and Eriksson, 2014):

$$T_\mathrm{e} = \eta_\mathrm{sc}\, \Pi_\mathrm{cyl}^{1-1/\gamma_\mathrm{a}}\, r_\mathrm{c}^{1-\gamma_\mathrm{a}} \left(\frac{q_\mathrm{in}}{c_\mathrm{p,a}} + T_\mathrm{im}\, r_\mathrm{c}^{\gamma_\mathrm{a}-1} \right) \tag{12a}$$

$$q_\mathrm{in} = \frac{W_\mathrm{f}}{W_\mathrm{f} + W_\mathrm{cyl}} q_\mathrm{HV}, \quad \Pi_\mathrm{cyl} = \frac{p_\mathrm{em}}{p_\mathrm{im}} \tag{12b}$$

Here η_sc is a model parameter, γ_a the ratio of specific heats for air, r_c is the compression ratio, and q_HV the fuel lower heating value. The cooling of the gas, before reaching the exhaust manifold, is modeled from (Eriksson, 2002):

$$T_\mathrm{em} = T_\mathrm{amb} + (T_\mathrm{e} - T_\mathrm{amb}) e^{-\frac{c_\mathrm{em,h}}{(W_\mathrm{cyl}+W_\mathrm{f})c_\mathrm{p,e}}} \tag{13}$$

Model parameter is $c_\mathrm{em,h}$, and $c_\mathrm{p,e}$ is the specific heat of the exhaust gas at constant pressure.

4.4 Torque

A large part of the modeling effort is devoted to modeling of the engine work. The engine torque, M_ice, is broken down into the components gross indicated torque M_ig, pumping torque M_pump, and friction torque M_fric:

$$M_\mathrm{ice} = M_\mathrm{ig} - M_\mathrm{pump} - M_\mathrm{fric} \tag{14}$$

As is customary in engine modeling and evaluation, work is normalized with engine displacement, V_D, and expressed in terms of the mean effective pressure (MEP). The relation between torque, M, and mean effective pressure is $4\pi M = V_\mathrm{D}\mathrm{MEP}$. $\mathrm{IMEP_g}$ is the gross indicated mean effective pressure (gross indicate that pumping losses are not included), PMEP is the pump mean effective pressure, and FMEP is the friction mean effective pressure. To be able to separate the different effects, data set B is used.

Indicated work

$\mathrm{IMEP_g}$ is modeled as in (Eriksson and Nielsen, 2014)

$$\mathrm{IMEP_g} = \eta_\mathrm{ig} \frac{q_\mathrm{HV}\, u_\mathrm{f}\, n_\mathrm{cyl}}{V_\mathrm{D}} \tag{15}$$

Achieving a good fit is a matter of modeling η_ig.

A modeling objective is to include the effect of the fuel-to-air ratio on the engine efficiency. The relation between the fuel-to-air ratio, the ratio of specific heats, and engine efficiency is described in (Heywood, 1988; Eriksson and Nielsen, 2014). An important question is how to include it in the model, and how that is done is an important contribution in this work.

The efficiency modeling is started from the efficiency of an ideal otto cycle, $1 - 1/r_\mathrm{c}^{\gamma-1}$, despite being a diesel engine. The reason for using it, is that it is a single parameter model, if the compression ratio r_c is considered given. To find a relation between efficiency and fuel-to-air ratio, the relation $\eta_\mathrm{ig,B} - (1 - 1/r_\mathrm{c}^{\gamma-1}) = 0$, is solved for γ for every datapoint in B, where $\eta_\mathrm{ig,B}$ is the indicated efficiency in the dataset. Figure 4 shows the solution, with γ drawn in circles, and a second order polynomial model of γ in ϕ is drawn in solid. The figure shows that the quadratic model can capture the trend and is like the trends found in literature. This motivates a model of the in-cylinder ratio of specific heats γ_cyl according to

$$\gamma_\mathrm{cyl}(\phi) = c_{\gamma,0} + c_{\gamma,1}\phi + c_{\gamma,2}\phi^2 \tag{16}$$

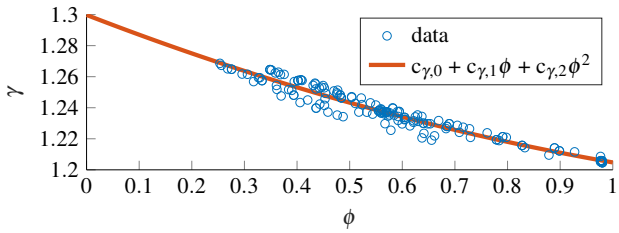

Figure 4. Drawn using circles is the γ that fulfills the relation $\eta_\mathrm{ig,B} - (1 - 1/r_\mathrm{c}^{\gamma-1}) = 0$ for every datapoint in B. Drawn in solid is a quadratic model of γ in ϕ.

The factor $\eta_\mathrm{cal}(N_\mathrm{ice}, u_\mathrm{f})$, is introduced. This gives the following structure for the indicated efficiency:

$$\eta_\mathrm{ig}(\phi, N_\mathrm{ice}, u_\mathrm{f}) = \left(1 - 1/r_\mathrm{c}^{\gamma_\mathrm{cyl}(\phi)-1}\right) \eta_\mathrm{cal}(N_\mathrm{ice}, u_\mathrm{f}) \tag{17}$$

To model η_cal, the same procedure as for γ is used. The equation $\eta_\mathrm{ig} - \eta_\mathrm{ig,B} = 0$ is solved for η_cal for every data point in B, $\eta_\mathrm{ig,B}$. Figure 5 shows the data plotted in circles, with constant coloring for constant engine speed. The data is plotted against fuel injection and engine speed. The figure clearly suggests a dependence on both fuel injection and engine speed. To model that, the model $\eta_\mathrm{cal} = c_\mathrm{cal,2}(u_\mathrm{f} - c_\mathrm{cal,1})^2 + c_\mathrm{cal,0}$ is fitted separately for the different engine speeds in the dataset, see solid lines in Figure 5. Figure 6 shows, drawn in circles, the evolution of the estimated parameters $c_\mathrm{cal,0}$, $c_\mathrm{cal,1}, c_\mathrm{cal,2}$ plotted against engine speed. In the same figure are different polynomial models of the trends plotted, which are estimated from the parameters using a least squares fit, and is used as a basis for modeling how the parameters change with engine speed.

The data and trends suggest the following modeling of the load and speed factor η_cal,

$$\eta_\mathrm{cal}(u_\mathrm{f}, N_\mathrm{ice}) = c_\mathrm{cal,2}(u_\mathrm{f} - c_\mathrm{cal,1})^2 + c_\mathrm{cal,0} \tag{18a}$$

$$c_\mathrm{cal,1} = c_\mathrm{cal,10} + c_\mathrm{cal,11} N_\mathrm{ice} \tag{18b}$$

$$c_\mathrm{cal,2} = c_\mathrm{cal,20} + c_\mathrm{cal,21} N_\mathrm{ice} + c_\mathrm{cal,22} (N_\mathrm{ice})^2 \tag{18c}$$

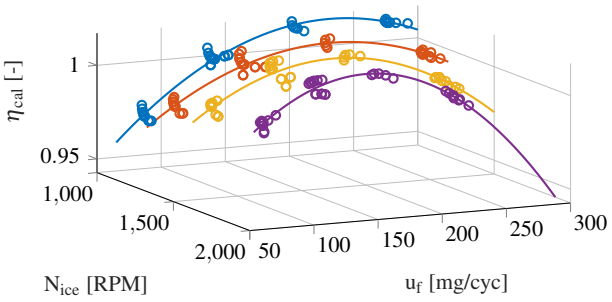

Figure 5. Drawn in circles is the solution to $\eta_{ig} - \eta_{ig,B} = 0$ for η_{ig}, calculated for every data point in B, $\eta_{ig,B}$. Drawn using solid lines is a least squares estimate of the model $\eta_{cal} = c_{cal,2}(u_f - c_{cal,1})^2 + c_{cal,0}$ for each speed-line.

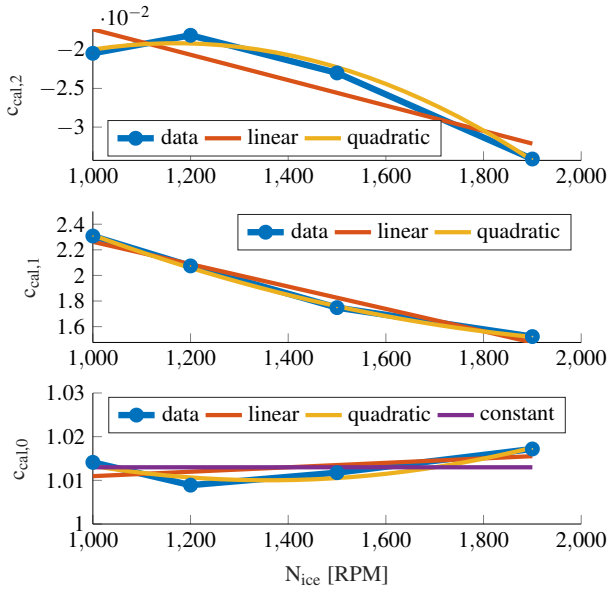

Figure 6. Evolution of $c_{cal,0}$, $c_{cal,1}$, $c_{cal,2}$, plotted against engine speed. Drawn using solid lines is the evolution modeled as polynomials in engine speed for different polynomial degree.

Pump work

The simplest model for the pump mean effective pressure is, PMEP $= p_{em} - p_{im}$. Dataset B gives a bias of 60 kPa for such a model for a least squares absolute error fit, also a linear model gives a bias, why an affine model is selected for the pumping work:

$$\text{PMEP}(p_{im}, p_{em}) = c_{\text{PMEP},0} + c_{\text{PMEP},1}(p_{em} - p_{im}) \quad (19)$$

with model parameters $c_{\text{PMEP},0}$ and $c_{\text{PMEP},1}$.

Friction work

A frequently used model for friction work is a second order polynomial in engine speed (Heywood, 1988). The available data in data set B does not show such a relation. Instead, data suggest the friction mean effective pressure can be modeled as a plane in engine speed, and fuel injection. A plot is available in Figure 7, in which circles

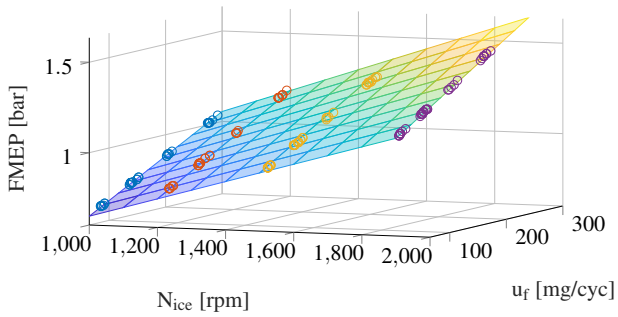

Figure 7. Drawn in circles is FMEP in data set B. Surface plot show the plane, FMEP $= c_{f,0} + c_{f,1}N_{ice} + c_{f,2}u_f + c_{f,3}u_f$, fitted from data.

show the mean effective pressure plotted against fuel injection and engine speed, and a surface plot shows a modeled plane. The model is formulated as follows

$$\text{FMEP}(u_f, N_{ice}) = c_{f,0} + c_{f,1}N_{ice} + c_{f,2}u_f + c_{f,3}u_f N_{ice} \quad (20)$$

in which $c_{f,0}$, $c_{f,1}$, $c_{f,2}$, and $c_{f,3}$ are model parameters.

4.5 Turbine

The turbine power is modeled based on (Eriksson, 2007), which lumps turbine power and the mechanical efficiency of the turbo shaft. By further introducing $c_{p,e}$ as the specific heat of the exhaust gas at constant pressure, and the subscript ats to indicate the aftertreatment system, the power is expressed as

$$P_t \eta_m = W_t c_{p,e} T_{em} \eta_t \left(1 - \Pi_t^{1-1/\gamma_e}\right) \quad (21a)$$

$$\Pi_t = p_{ats}/p_{em} \quad (21b)$$

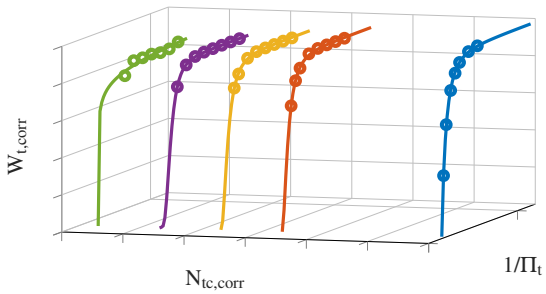

Figure 8. Drawn in circles is the corrected flow in the turbine map, dataset D. The data is plotted against corrected turbo speed $N_{tc,corr}$, and pressure ratio $1/\Pi_t$. Drawn in solid lines is the model $W_{t,corr} = k_0(1 - \Pi_t^{k_1})^{k_2}$ fitted to the different speed lines.

To obtain good accuracy, the square root turbine flow model (Eriksson and Nielsen, 2014) is used and extended with insights from the turbine map, dataset D. Figure 8 shows, drawn in circles, corrected flow $W_{t,corr} = W_t\sqrt{T_{em}}/p_{em}$, plotted against pressure ratio and corrected

turbo speed for dataset D, with constant coloring for constant turbocharger speed. For constant speed, the mass-flow model $W_{\mathrm{t,corr}} = k_0(1-\Pi_{\mathrm{t}}^{k_1})^{k_2}$ is fitted to the data. To settle upon flow equations, it is studied how the parameters k_0, k_1, and k_2 varies with turbocharger speed. A plot is shown in Figure 9, where circles show the value of the parameters for different speeds, and solid lines show different trend models. As is seen in the figure, k_1, and k_2, can be modeled as either linear or quadratic with reasonable results. The flow model is formulated as

$$W_{\mathrm{t,corr}} = k_0\left(1-\Pi_{\mathrm{t}}^{k_1}\right)^{k_2} \tag{22a}$$

$$k_0 = c_{00} + c_{02}\,N_{\mathrm{tc,corr}}^2 \tag{22b}$$

$$k_1 = c_{10} + c_{11}\,N_{\mathrm{tc,corr}} \tag{22c}$$

$$k_2 = c_{20} + c_{21}\,N_{\mathrm{tc,corr}} + c_{22}\,N_{\mathrm{tc,corr}}^2 \tag{22d}$$

$$N_{\mathrm{tc,corr}} = \frac{\omega_{\mathrm{tc}}}{\sqrt{T_{em}}} \tag{22e}$$

were c_i, $i = \{00,\ 02,\ 10,\ 11,\ 20,\ 21,\ 22\}$ are tuning parameters.

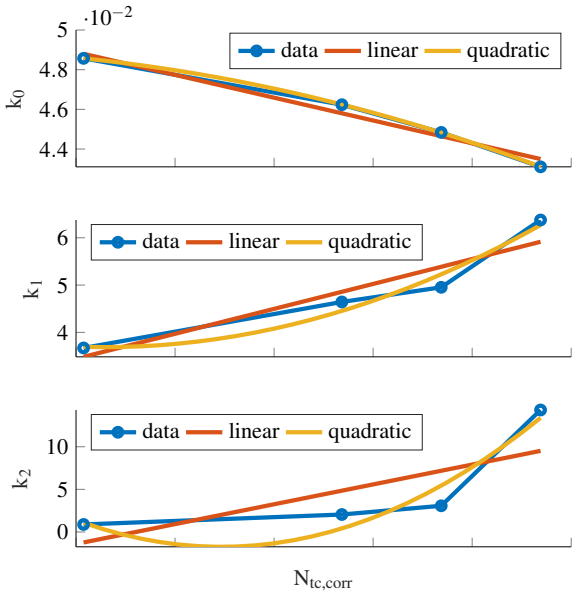

Figure 9. Circles show the evolution of parameters k_0, k_1, and k_2 plotted against turbocharger speed. Solid lines show first and second order polynomial models of the evolution.

The turbine efficiency is modeled based on the blade-speed-ratio (BSR), as defined in (Watson and Janota, 1982)

$$\mathrm{BSR} = \frac{\omega_{\mathrm{tc}}\,D_{\mathrm{t}}/2}{\sqrt{2\,c_{\mathrm{p,e}}\,T_{\mathrm{em}}\left(1-\Pi_{\mathrm{t}}^{1-\frac{1}{\gamma_{\mathrm{e}}}}\right)}} \tag{23}$$

Figure 10 shows the turbine efficiency of data set D plotted against blade-speed-ratio and corrected turbocharger speed. The data suggest the following model structure

$$\eta_t = \eta_{t,\max} - k_\eta\left(\mathrm{BSR}-\mathrm{BSR}_{\mathrm{opt}}\right)^2 \tag{24}$$

with parameters $\eta_{t,\max}$, k_η, and $\mathrm{BSR}_{\mathrm{opt}}$ speed dependent, a fit to the different speed lines is shown in the same figure using solid lines.

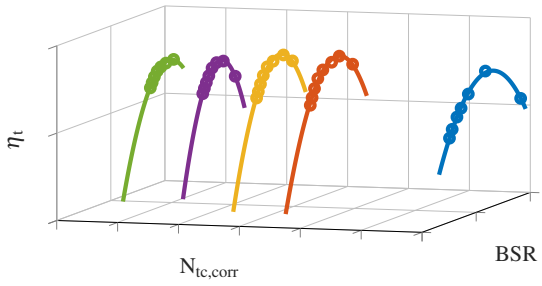

Figure 10. Circles show the turbine efficiency data from dataset D, plotted against corrected turbocharger speed, and blade-speed-ratio. Drawn in solid is a least fit of the model $\eta_t = \eta_{t,\max} - k_\eta\left(\mathrm{BSR}-\mathrm{BSR}_{\mathrm{opt}}\right)^2$ for each speed line.

Figure 11 shows the evolution of $\eta_{t,\max}$, k_η, and $\mathrm{BSR}_{\mathrm{opt}}$ with respect to speed. The data suggest that modeling of $\mathrm{BSR}_{\mathrm{opt}}$ could be linear or quadratic in speed. The model is formulated as

$$\mathrm{BSR}_{\mathrm{opt}} = c_{\mathrm{BSR},0} + c_{\mathrm{BSR},1}\,N_{\mathrm{tc,corr}} + \tag{25a}$$

$$c_{\mathrm{BSR},2}\,N_{\mathrm{tc,corr,II}}^2 \tag{25b}$$

$$\eta_{\mathrm{t,max}} = c_{\eta_t,0} + c_{\eta_t,1}\,N_{\mathrm{tc,corr}} + c_{\eta_t,2}\,N_{\mathrm{tc,corr}}^2 \tag{25c}$$

$$k_\eta = c_{\mathrm{max},0} + c_{\mathrm{max},1}\,N_{\mathrm{tc,corr}} \tag{25d}$$

where $c_{\mathrm{BSR},0}$, $c_{\mathrm{BSR},1}$, $c_{\mathrm{BSR},2}$, $c_{\eta_t,0}$, $c_{\eta_t,1}$, $c_{\eta_t,2}$, $c_{\mathrm{max},0}$, and $c_{\mathrm{max},1}$ are model parameters.

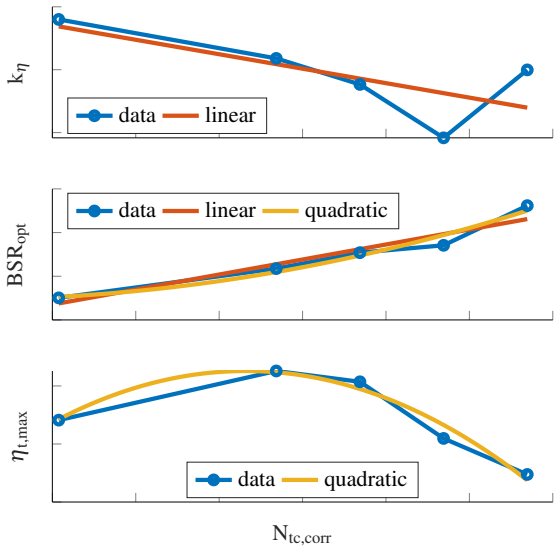

Figure 11. Circles show the evolution of parameters k_η, $\mathrm{BSR}_{\mathrm{opt}}$, and $\eta_{t,\max}$ plotted against turbocharger speed. Solid lines show first and second order polynomial models of the evolution.

4.6 Wastegate

Modeling of the wastegate follows that of the throttle, and the mass flow is modeled as

$$W_{\mathrm{wg}} = \frac{p_{\mathrm{em}}}{\sqrt{R_{\mathrm{e}}\, T_{\mathrm{em}}}} C_{\mathrm{D,wg}}\, A_{\mathrm{wg,max}}\, u_{\mathrm{wg}}\, \Psi_{\mathrm{wg}} \tag{26}$$

The flow head parameter Ψ_{wg} is modeled in the same way as the throttle, with the difference that γ_{a} is replaced by γ_{e}, and pressure ratio Π_{thr} replace by Π_{t}.

4.7 Compressor

The compressor modeling follows that of (Llamas and Eriksson, 2017) and uses the accompanied open-source parametrization tool *LiU CPgui* (Llamas and Eriksson, 2018). The model is a high-fidelity control-oriented compressor model intended to capture a full set of operating conditions. Parameterization data is dataset C. The development of the model component goes beyond the scope of this paper, but the compressor model paper describes the model well, and together with the freely available parameters and parametrization tool, the process is well documented.

5 Energy optimal control

To test the effect of including the air-to-fuel ratio on the energy optimal control, an OCP is presented and solved for the two cases when the effect is included and excluded. The problem is first solved for the presented model, and then using a fixed γ_{cyl} model. γ_{cyl} is then set so that the two solutions have the same average value for $1 - 1/r_{\mathrm{c}}^{\gamma_{\mathrm{cyl}}-1}$. The problem consists of using the least amount of energy to increase engine torque from the initial operating point, $\mathscr{X}_0$, at 200 Nm, to a final operating point $\mathscr{X}_f$, at 2400 Nm, and over the duration of the transient output 1 MJ of work. The engine speed is fixed at 1200 RPM, and the end time t_f is a free parameter. Fuel power is defined as $P_{\mathrm{f}} = q_{\mathrm{HV}} W_{\mathrm{f}}$, and energy consumption is its integral. Engine power is defined as $P_{\mathrm{ice}} = M_{\mathrm{ice}} N_{\mathrm{ice}} \pi/30$ and engine work as $E_{\mathrm{ice}} = \int P_{\mathrm{ice}}$. The engine model is represented by the differential equation $\dot{x} = f(x,u)$, and to avoid soot formation, the air-to-fuel ratio is restricted: $\lambda \geq 1.3$. The problem is formulated as:

$$\begin{aligned}
\min_{t_f,u} \quad & q_{\mathrm{HV}} \int_0^{t_f} W_f \, dt \\
\text{s.t.} \quad & \dot{x} = f(x,u), \\
& x(0) = \mathscr{X}_0,\ x(t_f) \geq \mathscr{X}_f, \\
& [0,0,0]^{\mathrm{T}} \leq u(t) \leq [280,1,1]^{\mathrm{T}}, \\
& \lambda(t) \geq 1.3, \\
& M_{\mathrm{ice}}(t_f) \geq 2400 \text{ Nm}, \\
& E_{\mathrm{ice}}(t_f) \geq 1 \text{ MJ}
\end{aligned} \tag{27}$$

As the end time is a free parameter, the first solution (including the effect of the air-to-fuel ratio) results in the end time 6.5 s, and the second in 4.3 s. Longer lines (blue) thus represent the solution with the original dynamics, and shorter lines (red) the solution with γ_{cyl} fixed. The dashed line shows the smoke limiter value of 1.3. The solutions are presented in Figure 12. For completeness, the figure shows all states and controls except p_{c} and u_{thr} as the throttle remains fully open in both cases. Of particular interest is the engine efficiency, defined as $\eta_{\mathrm{ice}}(t) = P_{\mathrm{ice}}(t)/P_{\mathrm{f}}(t)$, the indicated efficiency η_{ig}, and the air-to-fuel stoichiometric ratio λ. The fixed γ_{cyl} model pushes against the smoke limiter which makes the turbocharger spin up faster, thus reducing transient time and increases work output. Notice that this does not impair efficiency when the effect of the air-to-fuel ratio is excluded from the indicated efficiency model. Because of the higher engine efficiency, the fixed γ_{cyl} model can complete the transient faster, using less fuel. The original model on the other hand is forced to maintain a higher air-to-fuel ratio to maintain good efficiency. The air-to-fuel ratio is lowered at the end, which meets the constraint of engine torque, and at the same time reduces engine efficiency. The results show that the energy optimal control is significantly influenced by the air-to-fuel ratio, both quantitatively and qualitatively, which demonstrate the importance of including this effect in the model.

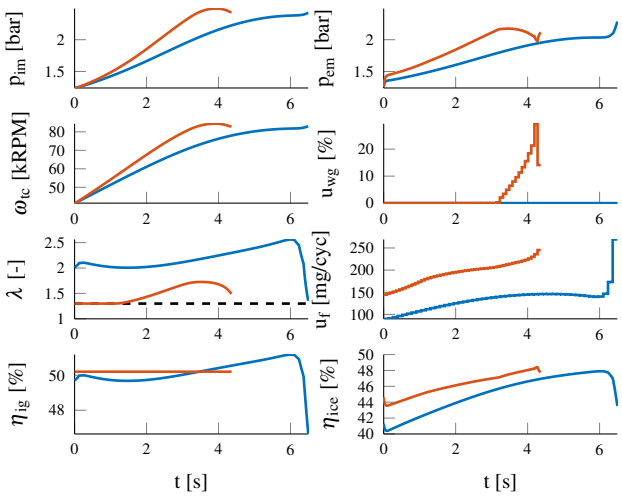

Figure 12. Solution to OCP (27). Longer lines (blue) show the solution to the problem for the presented model. Shorter lines (red) show the solution for a fixed γ_{cyl} model. The dashed line shows the smoke limiter.

6 Conclusions

A diesel engine model for energy optimal control is developed and documented, and available as open-source (Leek et al.). A method for estimating pressure sensor bias in experimental data is also presented. The model's intended use is to investigate the effect of the turbocharger selection on the energy optimal control. The model has a small number of states and controls to reduce the size of optimization problems. The dominating equations are based

on first principles for physically plausible extrapolation. The turbocharger model is detailed in order to accurately capture its effect on the air and fuel path dynamics. The engine efficiency model is dependent on the air-to-fuel ratio in order to include the effect of turbocharger dynamics on the combustion efficiency.

An optimal control problem is formulated and solved for the two scenarios of including the fuel-to-air ratio effect on the engine efficiency, versus excluding it. The results show that the air-to-fuel ratio has a significant quantitative and qualitative effect on the energy optimal transient control, and is an important aspect of turbocharger selection. This indicates that the model is fit for its intended use, but as the paper shows, the model's areas of use goes beyond that and to make it useful to others the development of the model is presented in full.

Acknowledgment

The work was financed by the *Swedish Agency for Innovation Systems* under the program LINK-SIC. The authors would like to thank Scania, especially Erik Höckerdal, Henrik Höglund and Björn Johansson for modeling discussions and data.

References

Joel Andersson. *A general-purpose software framework for dynamic optimization*. PhD thesis, PhD thesis, Arenberg Doctoral School, KU Leuven, Department of Electrical . . . , 2013.

Uri M Ascher and Linda R Petzold. *Computer methods for ordinary differential equations and differential-algebraic equations*, volume 61. Siam, 1998.

Jonas Asprion, Oscar Chinellato, and Lino Guzzella. Optimal control of diesel engines: Numerical methods, applications, and experimental validation. *Mathematical Problems in Engineering*, 2014, 2014.

John T Betts. *Practical methods for optimal control and estimation using nonlinear programming*. SIAM, 2010.

M. Diehl, H. G. Bock, H. Diedam, and P. B. Wieber. Fast direct multiple shooting algorithms for optimal robot control. *Lecture Notes in Control and Information Sciences*, 340:65–93, 2006. ISSN 01708643. doi:10.1007/978-3-540-36119-0_4.

Moritz Diehl. Numerical optimal control. Technical report, KU Leuven, 2011.

Kristoffer Ekberg, Viktor Leek, and Lars Eriksson. Modeling and validation of an open-source mean value heavy-duty diesel engine model. *Simul. Notes Eur.*, 28(4):197–204, 2018.

Lars Eriksson. Mean value models for exhaust system temperatures. *SAE Transactions*, pages 753–767, 2002.

Lars Eriksson. Modeling and control of turbocharged SI and DI engines. *Oil & Gas Science and Technology-Revue de l'IFP*, 62(4):523–538, 2007.

Lars Eriksson and Lars Nielsen. *Modeling and control of engines and drivelines*. John Wiley & Sons, 2014.

Lars Eriksson, Simon Frei, Christopher Onder, and Lino Guzzella. Control and optimization of turbocharged spark ignited engines. *IFAC Proceedings Volumes*, 35(1):283–288, 2002.

Gamma Technologies. GT-Power User's Manual. *GT-Suite Version 6.1*, 2004.

John B Heywood. *Internal combustion engine fundamentals*. McGraw-Hill Education, 1988.

Robin Holmbom and Lars Eriksson. Analysis and development of compact models for mass flows through butterfly throttle valves. Technical report, SAE Technical Paper, 2018.

Viktor Leek, Kristoffer Ekberg, and Lars Eriksson. LiU Diesel II - An open-source mean value engine model. Available at. `https://www.vehicular.isy.liu.se/Software/LiUDiesel2/`.

Xavier Llamas and Lars Eriksson. Control-oriented compressor model with adiabatic efficiency extrapolation. *SAE International Journal of Engines*, 10(4), 2017.

Xavier Llamas and Lars Eriksson. LiU CPgui: A toolbox for parameterizing compressor models. Technical report, Linköping University, SE-581 33, Linköping, Sweden, 2018.

Giorgio Mancini. *Automotive diesel engine transient operation: modeling, optimization and control*. PhD thesis, Università di Bologna, 2014.

Jorge Nocedal and Stephen Wright. *Numerical optimization*. Springer Science & Business Media, 2006.

Anil V Rao. A survey of numerical methods for optimal control. *Advances in the Astronautical Sciences*, 135(1):497–528, 2009.

Tielong Shen and Akira Ohata. Modeling and control design for automotive engines-with matlab engine simulator cd-rom. *ISBN 978e-4-339-04610-6*, 2011.

Martin Sivertsson and Lars Eriksson. Modeling for optimal control: A validated diesel-electric powertrain model. In *SIMS 2014-55th Scandinavian Conference on Simulation and Modelling*, pages 49–58. Linköping University Electronic Press, 2014.

Vaclav Smil. Diesel engine at 120 [numbers don't lie]. *IEEE Spectrum*, 54(2):24–24, 2017.

Johan Wahlström and Lars Eriksson. Modelling diesel engines with a variable-geometry turbocharger and exhaust gas recirculation by optimization of model parameters for capturing non-linear system dynamics. *Proceedings of the Institution of Mechanical Engineers, Part D: Journal of Automobile Engineering*, 225(7):960–986, 2011.

Neil Watson and Marian Janota. *Turbocharging the internal combustion engine*. Macmillan International Higher Education, 1982.